

Dexterous Manipulation with Underactuated Elastic Hands

Lael U. Odhner, *Member, IEEE*, and Aaron M. Dollar, *Member, IEEE*

Abstract—In this paper we show that it is possible to design underactuated robot hands capable of performing dexterous manipulation tasks, despite the fact that the motion of an underactuated hand is not fully constrained by its actuators. If a robot has elastic elements at its joints, then the velocity of the actuators can be mapped onto the velocity of the grasped object using elastic averaging. This mapping can be used to compute classical measures of manipulability for an underactuated hand. We also demonstrate that holonomically constrained grasps can be analyzed to determine the manifold of stable object configurations that can be reached from some initial grasp. This is especially useful for planar manipulation operations, such as twisting a knob or precision positioning. A prototype two-fingered planar underactuated hand is introduced, having the ability to stably grasp and manipulate objects within the hand.

I. INTRODUCTION

UNDERACTUATED robot hands are effective at grasping objects of uncertain size, shape, or location, because they are free to passively adapt to the shape of objects they contact. This reduces the need for precise sensing and control at each joint [1-4]. Hands having a small number of actuators are simpler to manufacture and ruggedize. At present, underactuated hands are used for immobilizing objects in fixed grasps, rather than dexterous within-hand manipulation. The barriers to developing simpler dexterous hands are partially practical issues of machine design, as it is clearly difficult to perform complex manipulation tasks with a limited set of actuators. However, the lack of complete mathematical tools for predicting underactuated hand behavior also hampers progress in this area. Specifically, better methods are needed for modeling the instantaneous kinematics of underactuated hands. Theoretical definitions of dexterity and assumptions about the nature of contact constraints can dominate the design requirements for dexterous hands [5]. Relaxing these assumptions to account for underactuated mechanisms will result in creative hand designs that use fewer actuators to perform dexterous tasks.

Standard methods of analysis fail to describe manipulation with underactuated hands because they describe all hand and object motion using the language of constraints. A model of a hand manipulating an object is typically broken up into several domains: actuator coordinates, joint coordinates, and object coordinates, depicted in Fig. 1. The local relationships

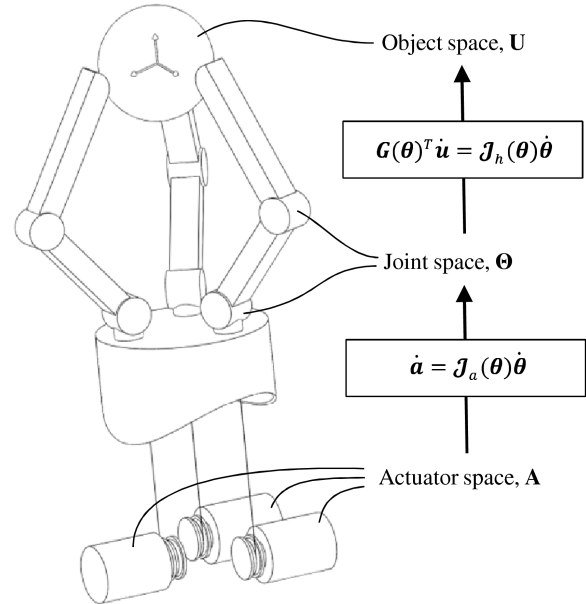


Fig.1. Manipulation can be described by examining how a change of actuator configuration, \mathbf{a} , impacts a change in the configuration of the hand joints, $\boldsymbol{\theta}$, and the configuration of the grasped object, \mathbf{u} .

between these coordinate systems are described by Pfaffian constraints, in the form of an actuator Jacobian, a hand Jacobian, and the grasp Jacobian. The properties of the constraints determine the capabilities of the robot hand. For example, an object is said to be graspable if the grasp Jacobian completely constrains all instantaneous motions of the object to instantaneous motions of the hand [6]. Similarly, an object is manipulable if all possible object motions can be realized by the actuator motions, as determined by the three constraint Jacobians. Scalar metrics are often used to quantify and optimize hand manipulability, such as the determinant or condition number of the constraint matrix between these coordinate systems [7, 8].

Underactuated hands do not nicely fit into the mold of constraint-based analysis. By definition, they have fewer actuators than joints, and consequently the Jacobian relating the actuator space to the hand configuration space is non-invertible. Only in power grasps is the motion of the underactuated hand and the grasped object fully constrained as a result of internal contact constraints. Past studies of dexterous motion in robots with unactuated joints have largely been limited to parallel manipulators, but these systems are still fully constrained by closed kinematic loops [9, 10].

In this paper, we will show that the lack of full-rank constraints defining hand actuation can in some cases be

This work was supported in part by National Science Foundation grant IIS-0952856 and by DARPA ARM-H, grant W91CRB-10-C-0141.

L.U. Odhner and A.M. Dollar are with the Department of Mechanical Engineering and Materials Science, Yale University, New Haven, CT USA (e-mail: {lael.odhner, aaron.dollar}@yale.edu).

accounted for by considering the principle of elastic averaging. That is, an elastic system will reach a predictable stable configuration when its motion is underconstrained. This principle, previously used to analyze planar compliant mechanisms [11], can be extended to underactuated hands systems to find the directional derivatives of grasped object motion with respect to actuator motion. Thus, traditional motions of instantaneous manipulability can be considered for underactuated hands.

In addition to the general problem of predicting instantaneous hand kinematics, we will present new methods for predicting the space of stable reachable configurations for a grasped object, if the contact constraints between the hand and object are holonomic. This subset of manipulation problems is particularly applicable to designing planar opposed fingers that need to perform one or two prototypical dexterous tasks, such as twisting knobs or unscrewing caps.

Finally, we will examine how the implications of these models line up with experimental results obtained from a modified planar version of the SDM hand [14]. The kinematics of the hand and the relative compliance of each joint strongly impact the nature of the dexterous tasks that can be performed.

The discussion in this paper will be focused on hands with multi-link serial fingers, such as the one depicted in Fig. 2. Each joint has an elastic element connected in parallel with the joint. Many underactuated hands incorporate elasticity of this kind. For example, the SARAH hand has similar kinematics to Hirose’s soft gripper, with the addition of springs throughout the finger linkages [1, 3]. Flexure-based underactuated hands such as the UB hands and the SDM hand also pair the basic Hirose kinematics with parallel stiffness at each joint due to the flexure mechanics [13, 14].

II. THE KINEMATICS OF UNDERACTUATED MANIPULATION

A robot’s ability to manipulate objects is often described in terms of local kinematics. Specifically, it is useful to characterize the range of motion that can be imparted to the object at any point. In this section, we will derive a general expression describing the mapping from the control inputs available to the hand (the actuator velocities) to the velocity space of a grasped object. The basic form of the result is similar to Gosselin and Quenouelle’s work [11], but it differs in several respects. Most notably, this derivation does not require a set of global unconstrained generalized coordinates. Because of this, non-holonomic contact constraints, common in manipulation problems, can be properly accounted for. Additionally, the approach taken here expresses the manipulation kinematics in the familiar form of a weighted pseudo-inverse, which is intuitive and notationally compact.

A. Terminology

We will define the actuator coordinates as a vector \mathbf{a} , the hand joint coordinates as $\boldsymbol{\theta}$, and the object body coordinates as \mathbf{u} . At any point, the local constraints between these

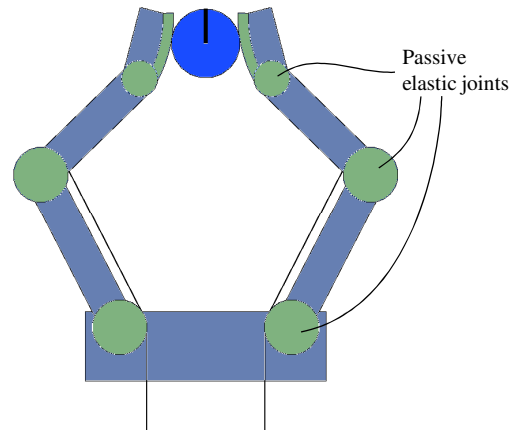


Fig. 2. A pair of underactuated, 3-link fingers holding a small object in a pinch grasp. The each finger is driven by a single tendon connected to the middle joint; the outer joint is purely passive.

coordinate systems are determined by three constraint Jacobians. Motion of the actuators can be related to motion of the joints using the actuation Jacobian, \mathbf{J}_a ,

$$\dot{\mathbf{a}} = \mathbf{J}_a(\boldsymbol{\theta})\dot{\boldsymbol{\theta}} \quad (1)$$

Relative motion of the hand in joint coordinates and the object in body coordinates is constrained through finger contacts by the hand Jacobian, \mathbf{J}_h , and the grasp matrix, \mathbf{G} ,

$$\mathbf{J}_h(\boldsymbol{\theta})\dot{\boldsymbol{\theta}} = \mathbf{G}(\boldsymbol{\theta})^T\dot{\mathbf{u}} \quad (2)$$

In this paper the grasp matrix will be written as a function of joint coordinates. In this paper we will presuppose that the object is in a graspable configuration, meaning that the grasp matrix has full row rank. Additionally, the grasp matrix will be written as a function of joint coordinates. A similar result could be derived if \mathbf{J}_h and \mathbf{G} were also functions of \mathbf{u} .

B. Constrained Hand Motions

The first step in characterizing the elastic behavior of the hand is to find a set of local coordinates describing the unconstrained motion of the hand and object, neglecting actuation constraints for the moment. We will assume that the hand configuration has been defined to eliminate any internal constraints, if the hand is a parallel mechanism. The grasping constraints will reduce the number of degrees of freedom in the configuration space of the hand/object system, $\boldsymbol{\theta} \times \mathbf{u}$,

$$[\mathbf{J}_h \quad -\mathbf{G}^T] \begin{bmatrix} \dot{\boldsymbol{\theta}} \\ \dot{\mathbf{u}} \end{bmatrix} = 0 \quad (3)$$

The constrained instantaneous motions of the hand and object will be represented as a vector $\dot{\mathbf{q}}$, and can be related to motion in the configuration space via a matrix \mathbf{R} , whose columns span the nullspace of the constraint matrix,

$$[\mathbf{J}_h \quad -\mathbf{G}^T] \begin{bmatrix} \dot{\boldsymbol{\theta}} \\ \dot{\mathbf{u}} \end{bmatrix} = [\mathbf{J}_h \quad -\mathbf{G}^T]\mathbf{R}\dot{\mathbf{q}} = 0 \quad (4)$$

The choice of the nullspace basis \mathbf{R} is arbitrary, and can be performed numerically for any constraint matrix. The dimension of $\dot{\mathbf{q}}$ is important, because the object cannot have

any more mobility than the contact constraints allow. This has a meaningful impact on hand design. For example, Fig. 3 shows a schematic comparison of a planar hand having two-link fingers and the three-link design of Fig. 2. There are two tendons driving the hand, so the dimension of $\dot{\mathbf{q}}$ should be greater than 2 if the two actuators are both going to be maximally useful for manipulation. The addition of two passive joints at the fingertips on the three-link hand ensures that the dimension of $\dot{\mathbf{q}}$ is 3, even if the fingertip contacts rigidly constrain the object to the distal links.

C. Static Equilibrium

The desired result of this derivation is a function mapping an arbitrary small change in actuation coordinates, $\delta\mathbf{a}$, onto a change in object coordinates, $\delta\mathbf{u}$. To do this, we will examine the conditions for static equilibrium change when a perturbation is applied to the configuration variables. For simplicity, we will sum the elastic forces on the hand, as well as any conservative forces on the grasped object, into a single potential energy function, $V(\boldsymbol{\theta}, \mathbf{u})$. In the case of a multi-link hand having rotary springs at the joints, the elastic energy of the hand will be a diagonal quadratic function of the joint angle vector. The equilibrium conditions for the system can be found by the principle of virtual work, in terms of the projected coordinates:

$$\begin{bmatrix} \mathbf{V}_\theta \\ \mathbf{V}_u \end{bmatrix} + \begin{bmatrix} \mathbf{J}_h^T \\ \mathbf{G} \end{bmatrix} \boldsymbol{\mu} + \begin{bmatrix} \mathbf{J}_a^T \\ 0 \end{bmatrix} \boldsymbol{\lambda} = 0 \quad (5)$$

Here the vector $\boldsymbol{\lambda}$ represents the forces satisfying the actuation constraints, and $\boldsymbol{\mu}$ is the vector of forces satisfying the grasping constraints. The vectors \mathbf{V}_θ and \mathbf{V}_u are the partial derivatives of the energy with respect to the object and hand coordinates. A small perturbation in actuator, hand and object coordinates must remain in equilibrium, which can be expressed via of the partial derivatives of (5),

$$\begin{bmatrix} \mathbf{V}_{\theta\theta} + \mathbf{S} & 0 \\ \mathbf{T} & \mathbf{V}_{uu} \end{bmatrix} \begin{bmatrix} \delta\boldsymbol{\theta} \\ \delta\mathbf{u} \end{bmatrix} + \begin{bmatrix} \mathbf{J}_h^T \\ \mathbf{G} \end{bmatrix} \delta\boldsymbol{\mu} + \begin{bmatrix} \mathbf{J}_a^T \\ 0 \end{bmatrix} \delta\boldsymbol{\lambda} = 0 \quad (6)$$

The actuator and grasp constraint forces must also vary to account for the perturbation in position. The matrices \mathbf{S} and \mathbf{T} describe the kinematic stiffness arising from the curvature in the constraints,

$$\mathbf{S}_{ij} = \sum_k \frac{\partial \mathcal{J}_{h,ki}}{\partial \theta_j} \boldsymbol{\mu}_k + \sum_l \frac{\partial \mathcal{J}_{a,li}}{\partial \theta_j} \boldsymbol{\lambda}_l \quad (7)$$

$$\mathbf{T}_{ij} = \sum_k \frac{\partial \mathbf{G}_{ik}}{\partial \theta_j} \boldsymbol{\mu}_k \quad (8)$$

In order to accurately account for the change in force in the unconstrained directions of motion, (6) must be projected onto the free space of motions using \mathbf{R} ,

$$\mathbf{R}^T \begin{bmatrix} \mathbf{V}_{\theta\theta} + \mathbf{S} & 0 \\ \mathbf{T} & \mathbf{V}_{uu} \end{bmatrix} \mathbf{R} \delta\mathbf{q} + \mathbf{R}^T \begin{bmatrix} \mathbf{J}_a^T \\ 0 \end{bmatrix} \delta\boldsymbol{\lambda} = 0 \quad (9)$$

Notice that the constraint forces due to grasping vanish, due to the relationship between \mathbf{R} and the grasp Jacobian from (4). This equation now contains a matrix which superficially resembles a stiffness term:

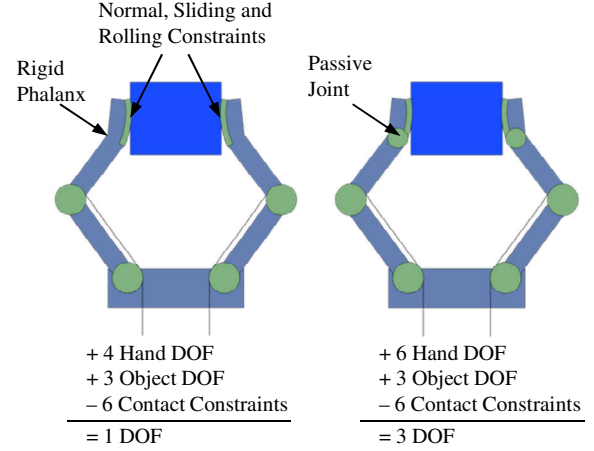


Fig. 3. A hand with two-link fingers (left) and a more dexterous three-link design (right). The dexterous design has a passive distal joint that allows motion even in the presence of “worst case” contact constraints.

$$\mathbf{K} = \mathbf{R}^T \begin{bmatrix} \mathbf{V}_{\theta\theta} + \mathbf{S} & 0 \\ \mathbf{T} & \mathbf{V}_{uu} \end{bmatrix} \mathbf{R} \quad (10)$$

\mathbf{K} is a pseudo-stiffness matrix because it is asymmetric when the contact constraints are non-holonomic, due to the lack of Hessian symmetry. However, if the contact constraints are holonomic, \mathbf{K} will be symmetric. The pseudo-stiffness can be singular under a variety of conditions. For example, the hand could have an insufficient number of independent elastic elements attached to the hand joints. Alternatively, the hand could buckle, if sufficiently large compressive forces are applied. In either of these cases, it will be impossible to predict the instantaneous motion of the system. If \mathbf{K} is invertible, then (10) can be rewritten to solve for $\delta\mathbf{q}$,

$$\delta\mathbf{q} = -\mathbf{K}^{-1} \mathbf{R}^T \begin{bmatrix} \mathbf{J}_a^T \\ 0 \end{bmatrix} \delta\boldsymbol{\lambda} \quad (11)$$

Equations (1) and (11) can now be used to find the corresponding change in actuator configuration, $\delta\mathbf{a}$,

$$\delta\mathbf{a} = -[\mathbf{J}_a \quad \mathbf{0}] \mathbf{R} \mathbf{K}^{-1} \mathbf{R}^T \begin{bmatrix} \mathbf{J}_a^T \\ 0 \end{bmatrix} \delta\boldsymbol{\lambda} \quad (12)$$

This equation can only be solved for $\delta\boldsymbol{\lambda}$ if the actuation constraints are linearly independent of each other, and linearly independent of the grasping constraints. In this case, then none of the eigenvectors in the nullspace of $\mathbf{R} \mathbf{K}^{-1} \mathbf{R}^T$ will appear in the matrix that needs to be inverted. Equation (12) can be solved and substituted back into (11),

$$\delta\mathbf{q} = \mathbf{K}^{-1} \mathbf{R}^T \begin{bmatrix} \mathbf{J}_a^T \\ 0 \end{bmatrix} \left([\mathbf{J}_a \quad \mathbf{0}] \mathbf{R} \mathbf{K}^{-1} \mathbf{R}^T \begin{bmatrix} \mathbf{J}_a^T \\ 0 \end{bmatrix} \right)^{-1} \delta\mathbf{a} \quad (13)$$

This can be substituted back into (4) to obtain the desired expression, the change in hand posture and object configuration as a function of $\delta\mathbf{a}$,

$$\begin{bmatrix} \delta\boldsymbol{\theta} \\ \delta\mathbf{u} \end{bmatrix} = \mathbf{R} \mathbf{K}^{-1} \mathbf{R}^T \begin{bmatrix} \mathbf{J}_a^T \\ 0 \end{bmatrix} \left([\mathbf{J}_a \quad \mathbf{0}] \mathbf{R} \mathbf{K}^{-1} \mathbf{R}^T \begin{bmatrix} \mathbf{J}_a^T \\ 0 \end{bmatrix} \right)^{-1} \delta\mathbf{a} \quad (14)$$

The relationship between hand/object configuration and actuator coordinates is in the form of a weighted pseudo-

inverse of the actuator constraint Jacobian, which is not unexpected. The pseudo-inverse is often posed in the form of a constrained minimization for the problem of differential motion [15]. The quantity to be minimized in this case is in fact the elastic energy of the system when the constraints are holonomic.

D. Discussion

We have shown that a kinematic relationship between the instantaneous motion of an underactuated hand and its actuators can be derived from the local conditions for elastic equilibrium. This relationship is written in terms of the constraint Jacobians commonly used to describe grasping, and holds for cases in which the contact constraints are holonomic or non-holonomic. It fails predictably when the matrices inverted in (11) and (13) are singular, and the possible causes of this singularity have been described in terms of known phenomena.

The significance of this result is that (14) provides directional derivatives locally connecting the manifold of actuator configurations to the manifold of object configurations, without requiring that a hand be fully actuated. Using this relationship, the manipulability of an object in an underactuated hand can be discussed, and quantified in terms of the eigenvalues of the pseudo-inverse matrix. In cases where the actuator velocities do not fully span all directions of object motion, it may be useful to consider manipulability on a lower-dimensional manifold, or to examine the implications that (14) has from the perspective of kinematic controllability [16].

It also bears mentioning that this derivation does not require that the hands have revolute joints. Many underactuated hands use flexures as hinges. As long as a parametric approximation such as can be found for the flexure behavior having as many independent energy storage modes as parameters, problems of manipulation with flexure-based mechanisms can also be addressed with this model. One such parametric approximation for Euler-Bernoulli flexures can be found in [17].

III. WORKSPACE ANALYSIS OF HOLONOMIC GRASPS

The previous section showed how to compute the local motions possible for a grasped object, irrespective of whether the grasping constraints were holonomic or not. This section deals with the problem of describing the global space of object configurations that can be reached from some initial grasp, if the contact constraints between the hand and some object are holonomic. Particularly, we are interested in planar manipulation operations between two opposed fingers, such as positioning a key or twisting a knob. The hand of Fig. 2, a modified version of the SDM hand, will be used as an example system. For hand/object systems with holonomic constraints, we will show that the region in which reachable object configurations are stable can be computed by boundary traversal or by grid mapping. The visualization tools developed are useful for understanding how design decisions impact the type of dexterous behaviors that an underactuated hand can produce.

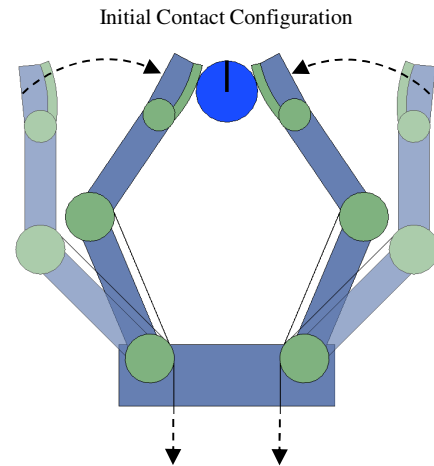


Fig. 4. An initial contact configuration for the hand/object system is found by adjusting the actuation constraints until the fingers make contact. The normal and rolling constraints are then applied to the model.

All hand modeling was performed using the Freeform Manipulator Analysis Toolbox, an extensible, object-oriented Matlab library developed by the authors. This toolbox has been released as open source software, along with the scripts used in this paper [18].

A. Holonomic Underactuated Manipulation

Many planar hand/object systems are holonomically constrained, if the grasping contacts can be modeled with idealized normal constraints, shear constraints and no-slip rolling constraints. In this case, it may be possible to construct a function mapping actuator coordinates to object coordinates for non-infinitesimal motions. The modified SDM hand under consideration has only two actuators, so an object pinched between the fingers will be able to move in a maximum of two directions locally. As a consequence, the reachable object configurations will all lie on some 2-dimensional manifold embedded in this space. The shape of this manifold can be computed by finding the object configuration which globally minimizes the energy in the system, subject to the actuator and grasping constraints.

B. Defining Grasping Constraints

The holonomic constraints between a hand and an object will be determined by the initial configuration in which the hand grasps the object. As shown in Fig. 4, this can be accomplished by modeling the free motion of the hand starting from its initial configuration, adjusting the actuator constraints until the fingers make initial contact with the object. The grasping constraints in this initial configuration are marginally satisfied at best, as the finger normal forces in this configuration are initially zero. The best way to assess the possible stability of this pinch grasp is to define the contact constraints in this configuration, and then to test the stability of several grasps in a neighborhood of the initial contact. In the case of the dexterous SDM hand, this meant defining the normal and rolling constraints between the fingertips and the cylindrical object, then perturbing the tendons inward slightly. As one might intuitively expect, the

object was found to be graspable when initially centered between the fingertips.

C. Stability Criteria

It is not enough to compute the manifold of kinematically reachable object configurations. On this manifold, some configurations will be stable and others will not. One principal criterion for stability is the validity of the grasping constraints. Discrete changes in hand configuration must also be considered, such as edges of contact surfaces or limits of travel on the joints. The object cannot, for example, roll off the tip of the finger and remain stable.

Compliance-based notions of stability are also important, because the underactuated system must rely on elastic restoring forces to remain in equilibrium in some directions [2]. This could be tested by bounding the magnitude of compliance matrix eigenvalues (non-zero eigenvalues representing directions along which elastic forces, rather than kinematic constraints, determine the reaction forces). Further, because components of the normal contact forces may be exerted by the elastic elements in the mechanism rather than an actuator, the ability of the hand to resist shear forces in some directions may be limited. We did not consider any large-disturbance or large-deformation instabilities; Gosselin and Birglen [12] and Herder and Kragten [19] both cover these cases in detail. In this paper, we considered a precision grasp to be stable if the grasping constraints are valid and the compliance is bounded.

D. Bounding the Stable Region

The stable space of reachable configurations was computed by traversing the boundary separating stable configurations from unstable configurations. Conveniently, one point on the boundary of the stable region is already known. The initial grasp of an object is marginally stable, as discussed in the Section IIIC. Starting from this point, we

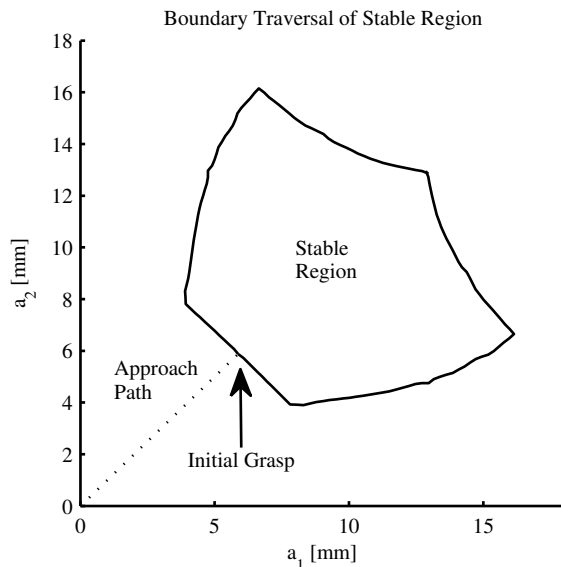


Fig. 5. The actuator configurations corresponding to stable grasps are encircled by the solid black line. The path in actuator space taken to approach the object is shown as a dashed line, and the intersection point is the initial grasp of the object.

Isometric Projection of Reachable Configurations

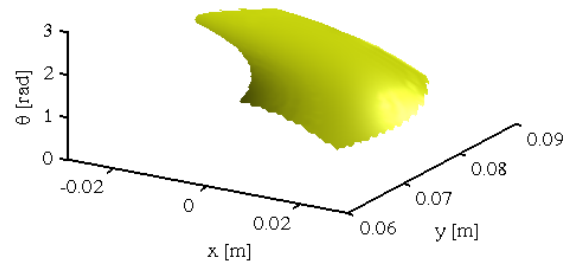
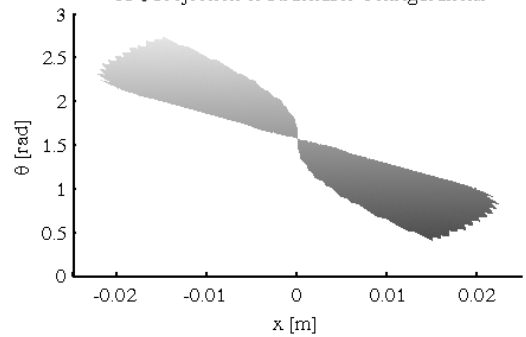


Fig. 6. The two-dimensional manifold of reachable object configurations, embedded in the object configuration space (x, y, θ) .

X- θ Projection of Reachable Configurations



X-Y Projection of Reachable Configurations

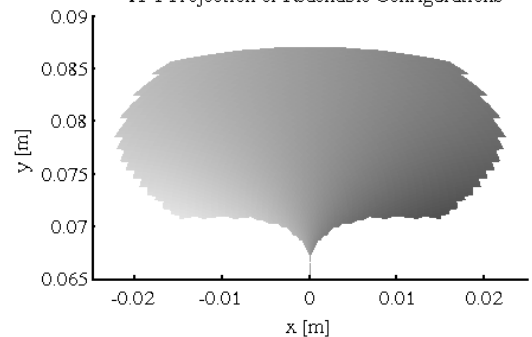


Fig. 7. The projection of the reachable configuration manifold onto the x - θ plane and the x - y plane.

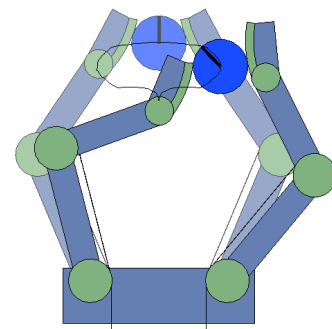


Fig. 8. The maximum lateral extent of motion possible in the hand is shown in the x - y plane, superimposed on the boundary of the stable object translations.

found two nearby actuator coordinates perturbed by $\Delta \mathbf{a}_1$ and $\Delta \mathbf{a}_2$. These offsets were selected so that one perturbed point lay inside the stable region and the other lay outside the stable region. A bisection search was then used to find the angle between these two perturbations corresponding to the marginally stable configuration, generating a new nearby point lying on the boundary. This iterative process was repeated for the two-actuator hand until a region of space was fully encircled. Figure 5 shows the resulting bounded region of actuator space. The axes of this plot correspond to the excursion of the two actuator tendons in millimeters. The boundary traversal algorithm does not determine whether there are any actuator configurations lie on interior of this region. To provide some assurance that this is not the case, the interior of the stable region was gridded and stability was verified at each point.

Figure 6 shows a surface plot of the stable, reachable object configurations, computed based on a grid of actuator coordinates taken from within the stable region. The edges of this manifold appear jagged because points on the interior of the stable region were sampled in a grid to make the surface. The true boundary is piecewise smooth, as it is in the actuator space. Figure 7 shows this same manifold from x - y and x - θ projections, shaded corresponding to the orientation of the object. Significant coupling between lateral motion and rotation of the object can be observed. To illustrate this coupling, the hand pose corresponding to maximum lateral motion is shown in Fig. 8 relative to the initial grasping pose.

E. Discussion

It is likely that the first dexterous underactuated hands will be designed to accommodate a small set of dexterous motion primitives, for realigning or reorienting objects that are too small to be grasped with the whole hand. Many of these primitives will likely be planar, holonomically constrained motions. Visualizing the reachable configurations of a grasped object could be useful for intuitively understanding how the hand geometry or the stiffness of each joint impacts the functioning of the hand. This method can also be used for optimization. If a realistic variety of object sizes and initial grasps are considered, it may be possible to find the hand whose reachable configuration manifold most closely approximates a set of desired object configurations.

IV. EXPERIMENTAL PROGRESS TOWARD A DEXTEROUS UNDERACTUATED HAND

This section presents an initial trial of the fingers of the SDM hand for use in dexterous tasks. The goal was to incorporate some of the lessons learned from the study of dexterous underactuated manipulation presented above and demonstrate useful dexterous manipulation with an underactuated hand. The fingertips on the original SDM fingers were rigid, as illustrated in Fig. 3. This design limited the mobility of the hand when an object was pinched between the fingertips. The modified fingers, shown in Fig. 9, have flexible tips made out of soft elastomer. This added mobility enables the fingers to rotate while retaining contact with a grasped object. Additionally, the original hand had

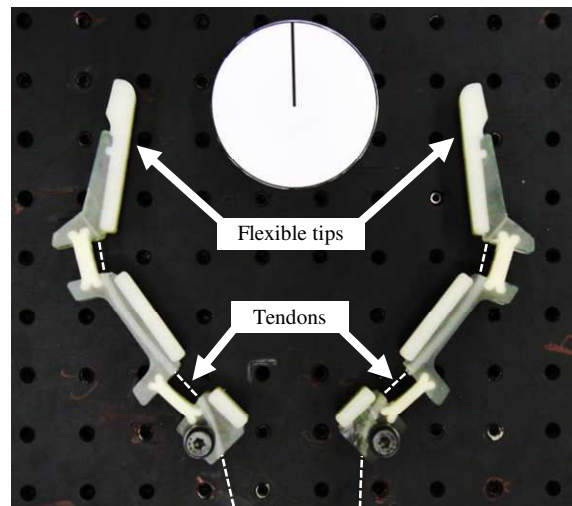


Fig. 9. A two-finger planar underactuated hand based on the SDM hand. The fingers of this hand have been modified to improve the hand's ability to manipulate objects grasped between the fingertips.

only one motor connected to all of the fingers through a differential mechanism. The modified hand incorporates one motor per finger, which represents a realistic compromise between simplicity and dexterity. The experimental hand was moderately successful at manipulating small objects. Fingertip grasping was notably more robust to small misalignments, and the hand was able to laterally reposition grasped objects. The range of motion was approximately 7.5 cm for grasped cylinders varying in diameter from 2.5 cm to the 7.5 cm cylinder shown moving in Fig. 10.

The observed manifold of reachable hand configurations was more or less one-dimensional (i.e. primarily left-right), rather than two-dimensional, as was hoped. The most likely reason for this is that the middle finger joint was significantly stiffer than the proximal joint. This design decision was made to maximize the swept area of the finger as it closes, so that off-center objects can be grasped. However, this also greatly increases the actuator force needed to pull the object further into the hand. The SDM fingers used here have a middle joint approximately 5.3 times as stiff as the proximal joint. When the actuator forces are modeled using this stiffness ratio, the force required to manipulate the object inward and outward to the extents of the workspace varies by a factor of 16.8. The shallowness of the experimentally reachable space of configurations is therefore most likely due to force saturation in the actuators. Future revisions of dexterous SDM fingers will re-distribute the joint stiffness to produce more uniform force requirements across the workspace.

The results of this first experiment in dexterous underactuated manipulation were encouraging. The modified SDM fingers are able to grasp objects between the fingertips, and to reposition objects within the hand. The range of motion and the kinds of motion possible (rotation vs. lateral motion) will be further developed to meet more specific functional requirements. It may also be useful to incorporate wrist movements in order to decouple in-hand rotation and translation without increasing hand complexity.

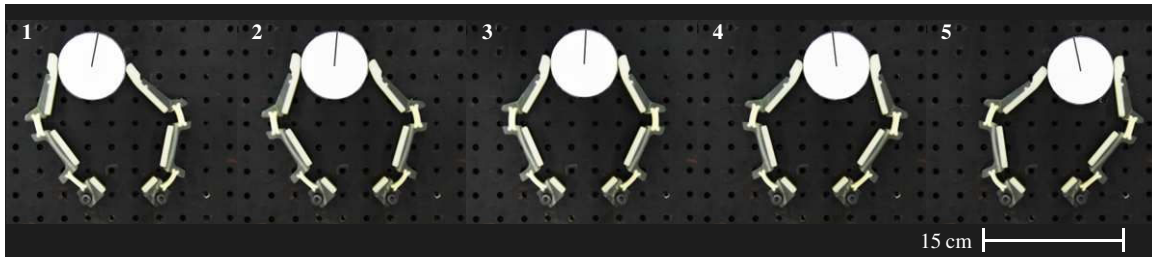


Fig. 10. A lateral motion of a pinched object from left to right, shown in sequence. The total motion of the object is 7.5 cm.

V. CONCLUSION

This paper has introduced modeling tools for assessing the degree to which underactuated hands are capable of performing dexterous manipulation tasks. These tools have been introduced at several levels of generality. First, we showed that for any underactuated elastic hand, it is possible to predict the instantaneous kinematics of the hand and grasped object by asserting that the elastic elements in the hand remain in quasi-static equilibrium when perturbed. This enables the application of classical manipulability criteria to underactuated hands. For the more limited set of circumstances where holonomic contact configurations can be guaranteed, or where the errors due to non-integrability of the constraints can be ignored, we demonstrated that it is possible to map out the configurations that can be reached from some initial grasp. This is particularly useful for the development of planar motion primitives for simplified hands. Lastly, we demonstrated a proof-of-concept experiment showing how an existing underactuated hand design can be modified to allow for in-hand manipulation. From this experiment, we identified one key factor – joint stiffness ratio – that strongly impacts the shape of the hand workspace.

The path to simple, dexterous robot hands lies in relaxing the assumptions that go into predictions of hand capability. When the capability criteria for dexterous hands are broadened, more creativity is allowed in the selection of hand mechanisms, including underactuated mechanisms. The tools outlined in this paper, and future improvements on these tools, will hopefully assist this push towards a balance between dexterity and simplicity.

REFERENCES

- [1] S. Hirose and Y. Umetani, "The Development of Soft Gripper for the Versatile Robot Hand," *Mechanism and Machine Theory*, Vol. 13, pp 351–359, 1978.
- [2] H. Hanafusa and H. Asada, "Stable prehension by a robot hand with elastic fingers," in *Robot Motion Planning and Control*, M. Brady, Ed., pp. 323-336. MIT Press, Cambridge, MA, 1982.
- [3] T. Laliberte, L. Birglen and C. Gosselin, "Underactuation in Robotic Grasping Hands," *Machine Intelligence & Robotic Control*, Vol. 4, No. 3, pp 1–11, 2002
- [4] A.M. Dollar and R.D. Howe, "Towards Grasping in Unstructured Environments: Grasper Compliance and Configuration Optimization", *Advanced Robotics*, vol. 19(5), pp. 523-543, 2005.
- [5] A. Bicchi, "Hands for Dexterous Manipulation and Robust Grasping : A Difficult Road Toward Simplicity," *IEEE Trans. on Robotics and Automation*, v. 16, n. 6, pp. 652-662, 2000.
- [6] D. Prattichizzo and A. Bicchi, "Dynamic Analysis of Mobility and Grasability of General Manipulation Systems," *IEEE Trans. on Robotics and Automation*, v. 14, n. 12, 1998.
- [7] M. Mason and K. Salisbury, *Robot Hands and the Mechanics of Manipulation*. MIT Press, Cambridge, MA, 1985.
- [8] T. Yoshikawa, "Manipulability of Robotic Mechanisms," *International Journal of Robotics Research*, v. 4, n. 3, 1985.
- [9] A. Bicchi and D. Prattichizzo, "Manipulability of Cooperating Robots with Unactuated Joints and Closed-Chain Mechanisms," *IEEE Trans. on Robotics and Automation*, v. 16, n. 4, 2000.
- [10] F.C. Park and J.W. Kim, "Manipulability and singularity analysis of multiple robot systems: A geometric approach," in *Proc. IEEE Int. Conf. on Robotics and Automation*, pp.1032-1037, 1998.
- [11] C. Quenouelle and C. Gosselin, "A quasi-static model for planar compliant parallel mechanisms," *ASME J. of Mechanisms and Robotics*, v. 1, n. 2, 2009.
- [12] L. Birglen and C. Gosselin, "Kinetostatic analysis of underactuated fingers," *IEEE Trans. on Robotics and Automation*, v. 20, n. 2, pp. 211-221, 2004.
- [13] F. Loti, P. Tiezzi, G. Vassura, L. Biagiotti, G. Palli, C. Melchiorri, "Development of UB Hand 3: Early Results," in *Proc. of the IEEE Int. Conf. on Robotics and Automation*, pp. 4499 –4504, 2005.
- [14] A. M. Dollar and R. D. Howe, "The Highly Adaptive SDM Hand: Design and Performance Evaluation," *International Journal of Robotics Research*, Vol. 29, No. 5, pp 585{597, 2010.
- [15] H. Asada and J.J.E. Slotine, *Robot Analysis and Control*. ch. 3.2, p. 69, Wiley Interscience, 1986.
- [16] R. Murray Z. Li S. Sastry, *A Mathematical Introduction to Manipulation*. ch. 7.2, p. 321, CRC Press, 1994.
- [17] L. Odhner and A. Dollar, "The smooth curvature flexure model: an accurate, low-dimensional approach for robot analysis," in *Robotics: Science and Systems 2010*, MIT Press, 2010.
- [18] L. Odhner and A. Dollar, "The Freeform Manipulator Analysis Toolbox" [Online]. Available <http://www.eng.yale.edu/grablab/fmat/>
- [19] J. Herder and G. Kragten, "A Platform for Grasp Performance Assessment in Compliant or Underactuated Hands," *J. Mechanical Design*, v. 132, n. 2, 2010.